JOURNAL OF GUIDANCE, CONTROL, AND DYNAMICS
Vol. 18, No. 2, March–April 1995

Reduced-Computation End-Game Steering Laws for Predictive Guidance

Roger L. Barron*
Barron Associates, Inc., Charlottesville, Virginia 22901-1444

A reduced-computation end-game (RCEG) steering law is derived for predictive guidance and simulated for a class of command guided weapons. The RCEG law considers maneuver control system response dynamics and variable axial and normal accelerations. It substantially reduces the guidance computational burden, while achieving accuracy comparable to that realizable with iterative predictive guidance (IPG). With IPG, each iteration requires numerical integration of vehicle equations of motion to predict the miss distance, whereas the RCEG law is noniterative and requires no integration. RCEG guidance uses closed-form miss distance estimates based upon lumped-parameter rotational and translational dynamics. Results of a six-degree-of-freedom simulation of a hypersonic intercept weapon system indicate that the RCEG law, compared with a representative form of IPG, has miss distances that are statistically similar to those of IPG but a computational burden smaller by a factor of approximately 36.

Nomenclature

A	= Eq. (18)
a	= divert maneuver acceleration
a_1, a_2, a_3	= divert maneuver accelerations over interval, $t - \Delta t + T_d \le t^* < t + T_d$, $t + T_d \le t^* < t + \Delta t + T_d$, and $t^* \ge t + \Delta t + T_d$, respectively
B	= Eq. (19); as subscript denotes ballistic
b	= binary variable, unity for formulation B, zero for formulation A
C	= Eq. (20); also, number of floating operations per integration interval; as subscript denotes guidance command
C_A, C_D	= axial force coefficient and drag coefficient, respectively
C_{N_α}	= partial derivative of normal-force coefficient with respect to α
C_{Y_β}	= partial derivative of sideforce coefficient with respect to β
D	= drag; as subscript denotes component along drag axis
$\underline{F}_0$	= Eqs. (A1–A3)
$\underline{\bar{F}}$	= Eq. (A4)
$f_{11}, \ldots, f_{33}$	= Eqs. (A5), ..., (A13)
$G_0, \ldots, G_3$	= Eqs. (57), ..., (60)
g	= local acceleration of gravity
$H_1, \ldots, H_4$	= Eqs. (38), (42), (47), and (54), respectively
H_{3a}, H_{3b}	= Eqs. (B7) and (B8), respectively
$H_{5a}, \ldots, H_{5c}$	= Eqs. (B9), ..., (B11)
I	= number of iterations per guidance decision
i	= subscript denoting axis in Earth-centered Earth-fixed system (except Δt_i = integration step)
$J_{1a}, \ldots, J_{2c}$	= Eqs. (B1), ..., (B6)
K	= guidance law gain, Eq. (70)
K_N	= coefficient of drag induced by normal force
K_Y	= coefficient of drag induced by sideforce
$k_{110}, \ldots, k_{330}$	= Eqs. (A14), ..., (A22)
L	= lift; as subscript denotes component along lift axis
m	= mass
N	= normal force
P	= subscript denoting guided vehicle
q	= dynamic pressure
R	= geocentric radius to flight vehicle
S	= reference area
T	= predicted time to go; as subscript denotes target vehicle
T_d	= transport delay
t	= time of guidance decision
t_f	= predicted final time (of closest approach)
t^*, t^{**}	= dummy variables of integration
V	= speed
W	= duration of command
x	= position coordinate in Earth-centered Earth-fixed system
Y	= sideforce; as subscript denotes component along sideforce axis
α, β	= aerodynamic angle of attack and angle of sideslip, respectively
γ	= flight-path climb angle relative to local horizontal
$\Delta( )$	= difference operator
$\delta p, \delta v$	= generalized position and velocity increments, respectively, produced by divert maneuver
δx	= position increment in Earth-centered Earth-fixed system produced by divert maneuver
$\underline{\varepsilon}$	= predicted miss distance
$\underline{\varepsilon}'$	= projection of $\underline{\varepsilon}$ on air-path axes
$\underline{\tilde{\varepsilon}}$	= $\underline{\varepsilon}$ excluding effect of guided-vehicle C_A term
η	= velocity divert angle
Λ, λ	= longitude and latitude, respectively
σ	= target-vehicle angular rate of coning oscillation
τ	= first-order time constant of guided-vehicle lumped-parameter divert acceleration response
χ	= flight-path heading angle relative to local North
Ω	= phase angle of target-vehicle coning oscillation
ω_E	= Earth sidereal rate about polar axis

Received April 8, 1993; revision received March 20, 1994; accepted for publication March 28,1994.

*President and Senior Research Scientist, 3046A Berkmar Drive. Member AIAA.

I. Introduction

END-GAME steering laws can be used during the final moments of flight of a guided intercept vehicle to achieve a desired final position (point of collision) and, in some cases, desired final velocity vector. The steering produced by classical proportional navigation may not be adequate for highly demanding end-game applications because it fails to account for dynamic lags in the interceptor maneuver control system and also because it assumes that the interceptor and target have no axial accelerations. Zarchan[1] provides a comprehensive treatment of proportional navigation and an

introduction to predictive guidance. Kim et al.[2] employ a kinematic algorithm to predict collision courses. Looze et al.[3] analyze use of target acceleration estimates in the end game. Cochran et al.[4] obtain analytical solutions to the nonlinear equations of relative motion for a constant-velocity target and an interceptor steered via a form of proportional navigation. Baba et al.[5] derive a collision course guidance law for the problem in which the interceptor and target axial accelerations are constant.

The maneuver control system dynamics can be particularly critical if one must meet stringent end-game requirements. A generally accepted approach for noniterative predictive guidance is to compute the unguided final miss distance, called the "zero-effort miss," via step-by-step numerical integration at each time of solution using modeled dynamics of the guided vehicle and its target.[1] The acceleration steering command is then set proportional to the zero-effort miss and usually is also made inversely proportional to the square of the predicted time to go T. Accuracy of single-pass predictive guidance may not be sufficient, however. On the other hand, brute-force, iterative guidance methods provide high accuracy but are computationally intensive. An example is IPG, which uses the acceleration command found from a suitable first iterate and makes a reprediction as its second iterate. Then, knowing the change in command from the first iterate to the second, and knowing also the resulting change in predicted miss, one can infer the sensitivity of one to the other and use that to compute the third iteration, and so forth. Each iteration can use knowledge of the vehicle acceleration limits and desirably will command maneuvers early in the end game so as to avoid or reduce terminal saturation. The iterated solutions for $T > 0$ can be expected to converge to zero final miss distance without producing terminal saturation if the interceptor has sufficient end-game time and maneuver authority; however, it is not uncommon to need as many as 50 iterations to achieve this convergence in demanding IPG applications.

Because an iterative sequence of predicted trajectories must be computed for each update, IPG requires approximately $C \times I \times T/\Delta t_i/\Delta t$ floating operations per second (FLOPS), in which Δt_i is the integration step size (s), and Δt is the interval (s) between guidance decisions. In an application summarized herein, end-game IPG use of a six-degree-of-freedom set of differential equations to characterize the translational and rotational responses of the guided vehicle, plus further degrees of freedom for its actuators, sensors, and inner-loop control law (autopilot), would require computing power of approximately 10^{10} floating operations per second (10 GFLOPS). A form of simplified IPG using only three-degree-of-freedom translational dynamics for this application imposes a throughput requirement of approximately 1.0 GFLOPS. A military fire control computer is usually occupied with many computations beyond those required by the steering law, including computations for sensor control, track estimation and prediction, control of multiple simultaneous engagements, and damage assessment, so the total processing burden can be much greater than these figures indicate. It is important to devise computationally feasible means for predictive guidance that sacrifice little, if any, performance in comparison with computationally intensive guidance methods.

To introduce the idea of RCEG predictive guidance, Sec. II treats a highly simplified exoatmospheric guidance problem. The interceptor is unpropelled (except for divert thrust), and it and its ballistic target are visualized as mass particles moving with known constant differential ballistic inertial accelerations. Moreover, it is assumed that steering accelerations of the guided vehicle are created without lag (that is, with infinite actuation bandwidth). The maneuver accelerations are assumed to be normal to the instantaneous velocity vector and to produce no change in tangential velocity. Errors in state and parameter estimation are ignored. Solutions with and without acceleration magnitude limits are obtained. Simple closed-form solutions are obtained for T and the components of the steering acceleration command.

Section III deals with a more general endoatmospheric RCEG guidance formulation that assumes that 1) the trajectory of the target is known from tracking data (the solution is formulated for the case of a target that is coning because of its tri-axial ballistics); 2) the acceleration response of the guided vehicle has the form of a pure transport delay followed by a first-order exponential rise (or fall) to the commanded acceleration level; 3) maneuver acceleration of the guided vehicle acts normal to its instantaneous velocity vector defined relative to the atmosphere; 4) induced (or crossflow) drag acting on the guided vehicle is proportional to the square of the resultant maneuver acceleration [for hypersonic speeds, this dependence may be closer to the 1.5 power (reviewer)]; and 5) the atmosphere density and guided vehicle aerodynamic coefficients, mass, and airspeed are constant over T. Errors in state and parameter estimation are again ignored. Closed-form solutions are derived for T and the steering acceleration command that will produce zero miss distance. This command may take the form of either a brief pulse or a constant over the time to go; in either case the command is readily subjected to saturation limits. A procedure is presented in Appendix B for treating the effects of axial acceleration changes over the T interval.

The RCEG solutions derived in Secs. II and III provide feedback steering laws that are tolerant of reasonable errors in physical realization of the commanded maneuver accelerations. The simple solution of Sec. II does not always degrade gracefully as acceleration response dynamics are introduced, and particular care must be exercised to verify its stability. The solution derived in Sec. III is more robust, and closed-loop stability has not been found to be an issue when using it. An attribute of the RCEG law in Sec. III is that it produces smooth variation of maneuver acceleration, which is known to aid in obtaining accurate state estimates. The RCEG laws are not asserted to be energy or time optimum. In weapon guidance, optimality vis-a-vis energy management is important when making midcourse trajectory adjustments, but the end-game imperative is to eliminate terminal error.

Section IV summarizes the results of Monte Carlo simulation runs. These used the RCEG solution of Sec. III and compared the performance of this steering law with that of the simplified IPG. The comparison considered end-game guidance of a representative hypervelocity terminal defense projectile intended to engage strategic and tactical threats.

II. Simple Case

If a guided vehicle (assumed to be unpropelled except for divert thrust) and its ballistic target are moving in a "flat-Earth," constant gravity field outside the atmosphere, the differential ballistic acceleration of these objects is constant. If divert maneuver accelerations of the guided vehicle can be created and removed instantly after known intervals of delay, if these accelerations have no magnitude limits and produce no changes in tangential velocity, and if there are no state estimation errors, exact solutions exist for T and the maneuver accelerations required to produce zero miss distance.

Let x_1, x_2, and x_3 represent rectangular position coordinates within a rotating Earth-centered Earth-fixed (ECEF) system having its origin at the Earth center, its $\boldsymbol{x}_1$ axis fixed in the equatorial plane at a reference meridian, its $\boldsymbol{x}_2$ axis fixed in the same plane at a meridian 90 deg. East of $\boldsymbol{x}_1$, and $\boldsymbol{x}_3$ directed along the North polar axis. Let this system rotate about $\boldsymbol{x}_3$ at the Earth sidereal rate ω_E. The equations of ballistic motion of an object outside the atmosphere can be written

$$\ddot{x}_{1_B} = 2\omega_E \dot{x}_2 + \omega_E^2 x_1 - x_1 g/R \tag{1}$$

$$\ddot{x}_{2_B} = -2\omega_E \dot{x}_1 + \omega_E^2 x_2 - x_2 g/R \tag{2}$$

$$\ddot{x}_{3_B} = -x_3 g/R \tag{3}$$

where

$$R = \left(x_1^2 + x_2^2 + x_3^2\right)^{\frac{1}{2}} \tag{4}$$

Let t_{f_B} denote the time of closest approach of the guided vehicle to its moving target, assuming both objects travel on purely ballistic paths. Then, defining $T_B = t_{f_B} - t$, and assuming T_B is small in the

intercept end game, the position of the target at t_{f_B} may be predicted by the second-order Taylor series

$$x_{T_i}(t_{f_B}) = x_{T_i}(t) + T_B\dot{x}_{T_i}(t) + \tfrac{1}{2}T_B^2\ddot{x}_{T_{i_B}}(t) \tag{5}$$

For the interceptor, one may similarly predict

$$x_{P_i}(t_{f_B}) = x_{P_i}(t) + T_B\dot{x}_{P_i}(t) + \tfrac{1}{2}T_B^2\ddot{x}_{P_{i_B}}(t) \tag{6}$$

The predicted zero-effort miss distance at t_{f_B} is then

$$\begin{aligned}\varepsilon_i(t_{f_B}) &= x_{T_i}(t_{f_B}) - x_{P_i}(t_{f_B}) \\ &= \Delta x_i(t) + T_B\Delta\dot{x}_i(t) + \tfrac{1}{2}T_B^2\Delta\ddot{x}_{i_B}(t)\end{aligned} \tag{7}$$

in which

$$\Delta x_i(t) = x_{T_i}(t) - x_{P_i}(t) \tag{8}$$

$$\Delta\dot{x}_i(t) = \dot{x}_{T_i}(t) - \dot{x}_{P_i}(t) \tag{9}$$

and when assumed constant from t to t_{f_B},

$$\Delta\ddot{x}_{i_B}(t) = \ddot{x}_{T_{i_B}}(t) - \ddot{x}_{P_{i_B}}(t) \tag{10}$$

(If T_B were large, the flat-Earth, constant-gravity assumption in Eqs. (5–7) would be invalid, and Keplerian motion would have to be considered.)

The RCEG computation derived later causes the three components of $\underline{\varepsilon}(t_{f_B})$ to be driven to zero by the guidance correction calculated at t. This correction will, in general, modify the time of closest approach, creating a new time to go

$$T = T_B + \Delta t_f = t_{f_B} + \Delta t_f - t \tag{11}$$

where Δt_f is the change in time of closest approach brought about by the guidance action.

For now, let us specify that the guidance correction $\ddot{x}_{P_c}$ will be computed as of time t, take effect as a step discontinuity at time $t + T_d$, continue for an interval Δt, then return instantaneously to zero at time $t + T_d + \Delta t$. The transport delay T_d results from the finite total time required to 1) update the tracking and guidance calculations, 2) communicate steering commands to the interceptor, and 3) provide for an assumed dead time in turn-on response of the maneuver subsystem reaction motors. A command that remains constant for two or more guidance intervals involves the T_d lag for the first interval only. The interval Δt should be the realistic minimum duration of guidance action; it cannot be less than the turnoff dead time of the reaction motors. The guided vehicle is assumed to move ballistically except during intervals of guidance action. (In Sec. III, the acceleration response model also includes the response of the autopilot loop used to control aerodynamic maneuver forces on the guided vehicle.)

Thus, for zero miss distance at the time of closest approach, one has, by superposition, assuming $\Delta\ddot{x}_{i_B}(t)$ remains constant from t to $t + T$,

$$\begin{aligned}&\varepsilon_i(t+T) = \varepsilon_i(t) + \Delta\varepsilon_i(t, t+T_d) + \Delta\varepsilon_i(t+T_d, t+T_d+\Delta t) \\ &\quad + \Delta\varepsilon_i(t+T_d+\Delta t, t+T) \\ &\quad = \Delta x_i(t) + T_d\Delta\dot{x}_i(t) + \tfrac{1}{2}T_d^2\Delta\ddot{x}_{i_B}(t) \\ &\quad + \tfrac{1}{2}(T - T_d - \Delta t)^2\Delta\ddot{x}_{i_B}(t) \\ &\quad + \Delta t\left[\Delta\dot{x}_i(t) + T_d\Delta\ddot{x}_{i_B}(t)\right] + \tfrac{1}{2}(\Delta t)^2\left[\Delta\ddot{x}_{i_B}(t) - \ddot{x}_{P_{i_c}}(t)\right] \\ &\quad + (T - T_d - \Delta t)\left\{\Delta\dot{x}_i(t) + T_d\Delta\ddot{x}_{i_B}(t)\right. \\ &\quad \left. + \Delta t\left[\Delta\ddot{x}_{i_B}(t) - \ddot{x}_{P_{i_c}}(t)\right]\right\} \\ &\quad = 0 \qquad (i = 1, 2, 3)\end{aligned} \tag{12}$$

This simplifies to the following command function

$$\begin{aligned}\ddot{x}_{P_{i_c}}(t) &= \frac{1}{\Delta t(T - T_d - \Delta t/2)} \\ &\times \left[\Delta x_i(t) + T\Delta\dot{x}_i(t) + \tfrac{1}{2}T^2\Delta\ddot{x}_{i_B}(t)\right]\end{aligned} \tag{13}$$

We see that the steering command is proportional to the predicted zero-effort miss. However, unlike conventional predictive guidance, which would set the command proportional to Eq. (7), the RCEG solution for this simple case involves gains T and $T^2/2$ on the velocity and acceleration terms, respectively, instead of T_B and $T_B^2/2$. Moreover, the overall gain, $1/\Delta t/(T - T_d - \Delta t/2)$, varies differently from the inverse square of time to go, which is the practice in conventional predictive guidance. The consequence of these differences is that this RCEG steering command gives single-correction nulling of the final miss distance, acting at its earliest opportunity to correct all of the predicted error. Conventional predictive guidance attempts only to correct a portion of this error over any given guidance interval Δt. The uncorrected portions tend to accumulate and require saturation commands as $T \to 0$. If the RCEG command is of a magnitude exceeding the actuation authority of the guided vehicle, the available maximum authority is used, and the solution is recomputed Δt later. Saturation commands early in the end game do not have the same adverse effect on terminal error as they do in the final moments.

In this solution, as in most end-game steering laws, it is necessary to estimate T. One approach is to employ an iterative algorithm. To govern the iterations, Lee[6] uses an objective function consisting of miss distance and time. Hull et al.[7] minimize normal-acceleration-weighted final time and, alternatively, final time. In highly demanding end-game guidance, the optimum answer is that for minimum miss distance. And iteration should be avoided, if possible, to reduce computational lag and complexity.

The RCEG steering solution in the present derivation yields a formula for T provided a suitable fourth condition is specified to supplement the three conditions prescribed by Eq. (13) for $i = 1, 2, 3$. A convenient fourth condition is that $\ddot{x}_{P_c}(t)$ will act along a perpendicular to the instantaneous velocity vector of the guided vehicle. [For exo-atmospheric engagements, the maneuver acceleration vector is usually directed perpendicular to the relative velocity vector between the target and guided vehicle (reviewer).] Therefore,

$$\ddot{x}_{P_{1_c}}(t)\dot{x}_{P_1}(t) + \ddot{x}_{P_{2_c}}(t)\dot{x}_{P_2}(t) + \ddot{x}_{P_{3_c}}(t)\dot{x}_{P_3}(t) = 0 \tag{14}$$

Generally, at least one component of $\underline{\dot{x}}_P(t)$ is nonzero. Dividing by this component, one obtains, from Eq. (14), if $\dot{x}_{P_1} \neq 0$,

$$\ddot{x}_{P_{1_c}}(t) = -\frac{\dot{x}_{P_2}(t)}{\dot{x}_{P_1}(t)}\ddot{x}_{P_{2_c}}(t) - \frac{\dot{x}_{P_3}(t)}{\dot{x}_{P_1}(t)}\ddot{x}_{P_{3_c}}(t) \tag{15a}$$

or, if $\dot{x}_{P_2} \neq 0$,

$$\ddot{x}_{P_{2_c}}(t) = -\frac{\dot{x}_{P_1}(t)}{\dot{x}_{P_2}(t)}\ddot{x}_{P_{1_c}}(t) - \frac{\dot{x}_{P_3}(t)}{\dot{x}_{P_2}(t)}\ddot{x}_{P_{3_c}}(t) \tag{15b}$$

or, if $\dot{x}_{P_3} \neq 0$,

$$\ddot{x}_{P_{3_c}}(t) = -\frac{\dot{x}_{P_1}(t)}{\dot{x}_{P_3}(t)}\ddot{x}_{P_{1_c}}(t) - \frac{\dot{x}_{P_2}(t)}{\dot{x}_{P_3}(t)}\ddot{x}_{P_{2_c}}(t) \tag{15c}$$

Setting the index i in Eq. (13) to the number that corresponds to an appropriate one of the relationships in Eqs. (15a–15c), the fourth condition takes the form

$$\begin{aligned}&\left[\Delta x_1(t) + T\Delta\dot{x}_1(t) + \frac{T^2}{2}\Delta\ddot{x}_{1_B}(t)\right]\dot{x}_{P_1}(t) \\ &+ \left[\Delta x_2(t) + T\Delta\dot{x}_2(t) + \frac{T^2}{2}\Delta\ddot{x}_{2_B}(t)\right]\dot{x}_{P_2}(t) \\ &+ \left[\Delta x_3(t) + T\Delta\dot{x}_3(t) + \frac{T^2}{2}\Delta\ddot{x}_{3_B}(t)\right]\dot{x}_{P_3}(t) = 0\end{aligned} \tag{16}$$

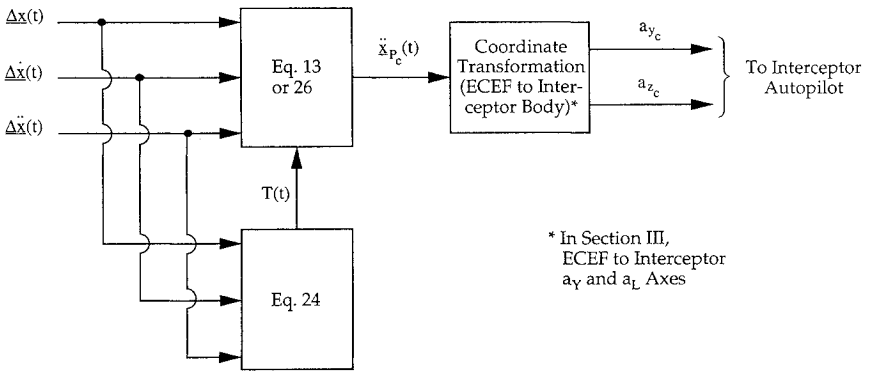

Fig. 1 Information flow in RCEG steering laws.

or

$$AT^2 + BT + C = 0 \tag{17}$$

where

$$A = \tfrac{1}{2}\left[\Delta\ddot{x}_{1_B}(t)\dot{x}_{P_1}(t) + \Delta\ddot{x}_{2_B}(t)\dot{x}_{P_2}(t) + \Delta\ddot{x}_{3_B}(t)\dot{x}_{P_3}(t)\right] \tag{18}$$

$$B = \Delta\dot{x}_1(t)\dot{x}_{P_1}(t) + \Delta\dot{x}_2(t)\dot{x}_{P_2}(t) + \Delta\dot{x}_3(t)\dot{x}_{P_3}(t) \tag{19}$$

$$C = \Delta x_1(t)\dot{x}_{P_1}(t) + \Delta x_2(t)\dot{x}_{P_2}(t) + \Delta x_3(t)\dot{x}_{P_3}(t) \tag{20}$$

Accordingly,

$$T = -\frac{B}{2A}\left(1 \mp \sqrt{1 - \frac{4AC}{B^2}}\right) \tag{21}$$

If $|4AC| \ll B^2$, and if the square root is subtracted from unity, the binomial theorem provides the approximation

$$T \doteq -\frac{B}{2A}\left(\frac{2AC}{B^2}\right) = -\frac{C}{B} \tag{22}$$

whence

$$\Delta t_f \doteq -\frac{\Delta x_1(t)\dot{x}_{P_1}(t) + \Delta x_2(t)\dot{x}_{P_2}(t) + \Delta x_3(t)\dot{x}_{P_3}(t)}{\Delta\dot{x}_1(t)\dot{x}_{P_1}(t) + \Delta\dot{x}_2(t)\dot{x}_{P_2}(t) + \Delta\dot{x}_3(t)\dot{x}_{P_3}(t)} - T_B \tag{23}$$

The general solution requires the negative sign ahead of the square root in Eq. (21) because if $C = 0$, the value of T must also be zero. Thus,

$$T = -\frac{B}{2A}\left(1 - \sqrt{1 - \frac{4AC}{B^2}}\right) \tag{24}$$

This value of time to go is used in Eq. (13), which then provides the three components of the RCEG steering command.

A variation on the preceding solution has proven to be useful for midcourse guidance. It specifies that the steering correction $\ddot{x}_{P_c}$ will continue unchanged from $t + T_d$ until $t + T$. Then, in place of Eq. (12),

$$\begin{aligned}\varepsilon_i(t+T) &= \varepsilon_i(t) + \Delta\varepsilon_i(t, t+T_d) + \Delta\varepsilon_i(t+T_d, t+T)\\ &= \Delta x_i(t) + T_d\Delta\dot{x}_i(t) + \tfrac{1}{2}T_d^2\Delta\ddot{x}_{i_B}(t)\\ &\quad + (T - T_d)\left[\Delta\dot{x}_i(t) + T_d\Delta\ddot{x}_{i_B}(t)\right]\\ &\quad + \tfrac{1}{2}(T - T_d)^2\left[\Delta\ddot{x}_{i_B}(t) - \ddot{x}_{P_{i_c}}(t)\right]\\ &= 0 \qquad (i = 1, 2, 3)\end{aligned} \tag{25}$$

whence one obtains the command function

$$\ddot{x}_{P_{i_c}}(t) = \frac{2}{(T - T_d)^2}\left[\Delta x_i(t) + T\Delta\dot{x}_i(t) + \tfrac{1}{2}T^2\Delta\ddot{x}_{i_B}(t)\right] \tag{26}$$

Note that this alternative design can have the same solution for T, Eq. (24), as does the command function of Eq. (13). For endo-atmospheric guidance using Eq. (26), $\Delta\ddot{x}_{i_B}$ should be estimated for the complete path to go. Polynomial neural networks[8,9] have been used successfully for this purpose. The steering law of Eq. (26) is also valuable for RCEG steering when $T_d \le T < \Delta t$.

Figure 1 presents the information flow used in the RCEG steering laws.

A variation on the solutions of Eqs. (13) and (26) is that in which the magnitude of the corrective acceleration is predetermined, whereas its polarity and duration are to be calculated. Let $W_i(t)$ denote the command duration for axis i, and note that $W_i(t) > 0$. Continuing to assume that the guided vehicle mass is constant, one obtains

$$\begin{aligned}\ddot{x}_{P_{i_c}}(t) &= \frac{1}{W_i(t)(T - T_d - W_i(t)/2)}\\ &\quad \times \left[\Delta x_i(t) + T\Delta\dot{x}_i(t) + \tfrac{1}{2}T^2\Delta\ddot{x}_{i_B}(t)\right]\end{aligned} \tag{27}$$

whence

$$\begin{aligned}W_i(t) &= (T - T_d)\\ &\quad \times \left[1 - \sqrt{1 - \frac{2\left[\Delta x_i(t) + T\Delta\dot{x}_i(t) + \tfrac{1}{2}T^2\Delta\ddot{x}_{i_B}(t)\right]}{(T - T_d)^2\ddot{x}'_{P_{i_c}}(t)}}\right]\end{aligned} \tag{28}$$

where $\ddot{x}'_{P_{i_c}}(t)$, the corrective acceleration, has a given magnitude and a polarity prescribed by Eq. (27). The solution for T can again be that of Eq. (24). The case of variable mass also has a closed-form $W_i(t)$ solution, not presented here.

In general, the steering laws of Eqs. (13) and (27) will use more maneuver energy in the presence of estimation errors than the solution of Eq. (26), whereas Eq. (26) will produce greater miss distance. In the end game, miss distance is the greater concern.

III. General Case

Assuming, as before, perfect knowledge of the states of both objects, the other assumptions of Sec. II will now be relaxed or modified as follows. We suppose the guided vehicle and its target to be moving inside the atmosphere and that the guided vehicle uses aerodynamic forces to maneuver. The target object is viewed as descending on a nominally ballistic trajectory but exhibiting small pitch and yaw oscillations that produce a coning motion having slowly varying total aerodynamic angle and constant frequency. The differential ballistic acceleration of the two objects is updated at each decision time during the engagement to account for the fact that aerodynamic steering of the guided vehicle produces induced drag that alters its ballistic acceleration. Of particular importance to synthesis of a stable feedback law, the derivation now makes no assumption that maneuver accelerations of the guided vehicle can be created and removed instantaneously. High-order characteristics of the autopilot loops of the guided vehicle, including body rotational dynamics, the dynamics of actuators and sensors, and computational lags, are treated as lumped-parameter effects. Results of detailed simulations have verified that the lumped-parameter characterization provides a noniterative feedback law equivalent in its performance to iterative predictive guidance and tolerant of off-nominal values of system parameters.

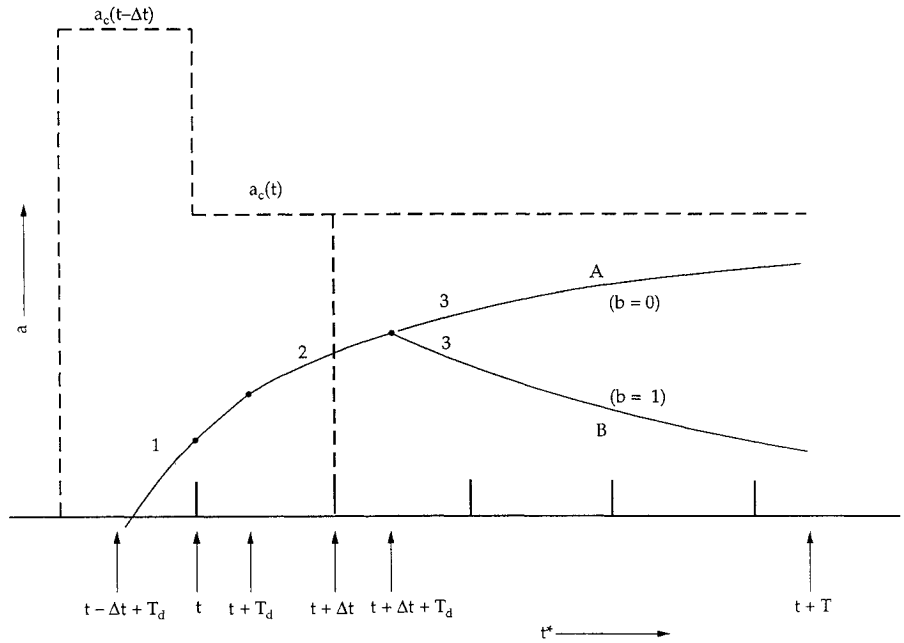

Fig. 2 Hypothetical acceleration responses to steering command at t.

The first step in the more general RCEG steering law derivation is to set forth the endo-atmospheric equations of motion. From Appendix A these can be expressed as

$$\ddot{\underline{x}} = \underline{F}_0 + \frac{1}{m}\underline{\underline{F}}\begin{bmatrix} D \\ Y \\ L \end{bmatrix} \tag{29}$$

where D, Y, and L are defined in air-path (wind) axes; $\underline{\underline{F}}$ is a rotation matrix defined (Appendix A) in terms of latitude, longitude, and trajectory climb angle γ and heading angle χ; and $\underline{F}_0$ is a vector defined in Appendix A in terms of $\underline{x}$, $\dot{\underline{x}}$, latitude, and longitude.

For the guided vehicle, $\ddot{\underline{x}}$ becomes $\ddot{\underline{x}}_P$, $\underline{F}_0$ becomes $\underline{F}_{0_P}$, $\underline{\underline{F}}$ is denoted $\underline{\underline{F}}_P$, and, restricting attention to small α and β, and assuming a quadratic drag polar,

$$D = q_P S_P\left(C_A - K_Y\beta^2 + K_N\alpha^2\right) \tag{30}$$

$$Y = q_P S_P(K_Y + C_A)\beta \tag{31}$$

$$L = q_P S_P(K_N - C_A)\alpha \tag{32}$$

in which q_P is dynamic pressure ($q_P = \frac{1}{2}\rho_P V^2$, where ρ_P is atmosphere density at the altitude of the guided vehicle and V is the airspeed of the guided vehicle), S_P is a constant reference area, and $K_Y = C_{Y_\beta}$ and $K_N = C_{N_\alpha}$ are nondimensional sideforce and normal-force partial derivatives with respect to β and α, respectively. Perfect knowledge of C_A, K_Y, and K_N is here assumed.

For the target

$$\ddot{\underline{x}}_T = \underline{F}_{0_T} + \frac{q_T S_T}{m_T}\underline{\underline{F}}_T\begin{bmatrix} C_{D_T} \\ C_{N_{\alpha_T}}\alpha_T\sin(\sigma t + \Omega) \\ C_{N_{\alpha_T}}\alpha_T\cos(\sigma t + \Omega) \end{bmatrix} \tag{33}$$

where C_{D_T} is the drag coefficient, $C_{N_{\alpha_T}}$ is the partial derivative of the normal force coefficient with respect to angle of attack, σ is the coning angular rate, and Ω is the coning phase angle at $t = 0$. The problem of estimating target parameters is not considered here.

Assuming that the guided vehicle is axisymmetric, $K_Y = -K_N$. Solving Eqs. (31) and (32) for β and α, respectively, and substituting into Eq. (30) divided by m, one obtains

$$D/m = \frac{q_P S_P C_A}{m_P} + \frac{K_N m_P\left(a_Y^2 + a_L^2\right)}{q_P S_P(K_N - C_A)^2} \tag{34}$$

in which $a_Y = Y/m_P$ and $a_L = L/m_P$. Thus, for this vehicle

$$\ddot{\underline{x}}_P = \underline{F}_{0_P} + \underline{\underline{F}}_P\begin{bmatrix} \dfrac{q_P S_P C_A}{m_P} + \dfrac{K_N m_P\left(a_Y^2 + a_L^2\right)}{q_P S_P\left(K_N - C_A\right)^2} \\ a_Y \\ a_L \end{bmatrix} \tag{35}$$

We next expand the predicted zero-effort miss distance in a corrected second-order Taylor series

$$\varepsilon(t_{f_B}) = \Delta\underline{x}(t) + T\Delta\dot{\underline{x}}(t) + \tfrac{1}{2}T^2\Delta\ddot{\underline{x}}_B(t) + \delta\underline{x}_{T_B}\left(t_{f_B}\right) - \delta\underline{x}_{P_B}\left(t_{f_B}\right) \tag{36}$$

where the last two terms are the contributions of changes in the ballistic accelerations of the threat and guided vehicle, respectively, over the interval between t and t_{f_B}. [Ideally, the predicted ballistic miss distance, Eq. (36), will be eliminated by implementation of a perfect guidance decision made at t.] In the present, more general, treatment, there are three major topics not treated in Sec. II: 1) use of the endo-atmospheric equations of motion, Eqs. (33) (including coning) and (35); 2) periodic updating of $\Delta\ddot{\underline{x}}_B(t)$ in Eq. (36) to account for a nonzero difference between the last two terms in the prediction; and 3) a more complete lumped-parameter modeling of guided-vehicle responses to a_Y and a_L commands.

Hypothetical incremental motion of the guided vehicle in response to a_Y and a_L commands at t is shown by the plot in Fig. 2, where two solutions are illustrated. In formulation A, it is assumed that the guided-vehicle divert accelerations respond (with lag) to commands a_{Y_c} and a_{L_c} that are constant over the interval $(t, t + T)$ and produce zero predicted miss distance. In formulation B, it is assumed that the predicted final error is nulled by a guidance command that is confined to the interval $(t, t + \Delta t)$. Because both the computation algorithm and the realization of the computed guidance actions for these formulations are, in the real world, imperfect, it is likely that further guidance actions will become appropriate at $t + \Delta t$, $t + 2\Delta t$, and so forth, with each subsequent action chosen to use the latest tracking information available at the relevant time of decision and null the residual predicted final error from all previous actions. Note that formulation A will usually produce smaller acceleration commands than formulation B.

The lumped-parameter solution for the autopilot-loop acceleration response of the general RCEG steering solution is characterized by a transport delay T_d as in Sec. II, followed by a linear first-order response having a time constant τ (assumed to have the same value

for thrust growth and decay). The first-order portion of the response model represents the assumed behavior of the interceptor acceleration subsequent to the transport delay. The guidance update interval Δt is usually much less than τ, but always at least equal to T_d. It is assumed that the response to a sequence of guidance commands can be calculated via superposition. As shown in Fig. 2, a decision is made at time t concerning the air-path axes (wind-axes) acceleration command $a_c(t)$ used in this analysis to represent, in turn, $a_{D_c}(t)$, $a_{Y_c}(t)$, and $a_{L_c}(t)$. A measurement at time t of the existing divert acceleration provides $a(t)$; moreover, it is known that the system is responding to its prior command, $a_c(t-\Delta t)$, for which the delayed response of the system began at time $(t-\Delta t+T_d)$ at the acceleration level then existing. During the interval $(t, t+T_d)$ the system continues to move along arc no. 1, for which the equation of divert acceleration response is

$$a_1(t^*) = a_c(t-\Delta t) + H_1 \exp\left(-\frac{t^*}{\tau}\right) \tag{37}$$

where

$$H_1 = [a(t-\Delta t+T_d) - a_c(t-\Delta t)]\exp\left(\frac{t-\Delta t+T_d}{\tau}\right) \tag{38}$$

In general, $a_c(t) \neq a_c(t-\Delta t)$, and the acceleration $a(t^*)$ moves along a new path, arc no. 2, in Fig. 2 beginning at time $(t+T_d)$. Accordingly, over the interval $(t+T_d, t+T)$ in formulation A,

$$a_2(t^*) = a_c(t) + [a(t+T_d) - a_c(t)]\exp\left(-\frac{t^*-t-T_d}{\tau}\right) \tag{39}$$

However, $a(t+T_d)$ is not observable at time t, although it is readily predicted by setting $t^* = t+T_d$ in Eq. (37),

$$a(t+T_d) = a_c(t-\Delta t) + H_1 \exp\left(-\frac{t+T_d}{\tau}\right) \tag{40}$$

and therefore Eq. (39) takes the form

$$a_2(t^*) = a_c(t) + H_2 \exp\left(-\frac{t^*}{\tau}\right) \tag{41}$$

in which

$$H_2 = H_1 + [a_c(t-\Delta t) - a_c(t)]\exp\left(\frac{t+T_d}{\tau}\right) \tag{42}$$

In formulation A it is assumed, for the purpose of calculating $a_c(t)$, that the divert acceleration moves along arc no. 2 from time $(t+T_d)$ until the threat is intercepted at $(t+T)$. In formulation B, however, it is assumed that the divert acceleration decays toward zero beginning at time $(t+\Delta t+T_d)$. In both formulations one solves for the guidance acceleration command $a_c(t)$ that nulls the final error.

It is evident that formulation A is a special case of formulation B, and it is convenient to employ a binary variable b that is unity for B, but zero for A, and vice versa for $\bar{b}$. Accordingly, the guidance acceleration for $t^* \geq t+\Delta t+T_d$ becomes

$$a_3(t^*) = \bar{b}a_2(t^*) + b \times [a(t+\Delta t+T_d)]\exp\left(-\frac{t^*-t-\Delta t-T_d}{\tau}\right) \tag{43}$$

Although $a(t+\Delta t+T_d)$ is not observable at time t, by setting $t^* = t+\Delta t+T_d$ in Eq. (41), one has the prediction

$$a(t+\Delta t+T_d) = a_c(t) + H_2 \exp\left(-\frac{t+\Delta t+T_d}{\tau}\right) \tag{44}$$

and therefore Eq. (43) becomes

$$a_3(t^*) = \bar{b}a_2(t^*) + b \times \left[a_c(t) + H_2 \exp\left(-\frac{t+\Delta t+T_d}{\tau}\right)\right] \times \exp\left(-\frac{t^*-t-\Delta t-T_d}{\tau}\right) \tag{45}$$

Substituting Eq. (41) for $a_2(t^*)$

$$a_3(t^*) = \bar{b}a_c(t) + H_3 \exp\left(-\frac{t^*}{\tau}\right) \tag{46}$$

wherein (because $\bar{b}+b=1$)

$$H_3 = H_2 + b \times [a_c(t)]\exp\left(\frac{t+\Delta t+T_d}{\tau}\right) \tag{47}$$

The generalized velocity increment produced by divert action over the interval (t, t^{**}) is thus

$$\delta v(t^{**}) = \int_t^{t+T_d} a_1(t^*)\,dt^* + \int_{t+T_d}^{t+\Delta t+T_d} a_2(t^*)\,dt^* + \int_{t+\Delta t+T_d}^{t^{**}} a_3(t^*)\,dt^* \tag{48}$$

The first integral in Eq. (48) is

$$\int_t^{t+T_d} a_1(t^*)\,dt^* = [a_c(t-\Delta t)]T_d - \tau H_1 \times \left[\exp\left(-\frac{t+T_d}{\tau}\right) - \exp\left(-\frac{t}{T}\right)\right] \tag{49}$$

The second integral is

$$\int_{t+T_d}^{t+\Delta t+T_d} a_2(t^*)\,dt^* = [a_c(t)]\Delta t - \tau H_2 \times \left[\exp\left(-\frac{t+\Delta t+T_d}{\tau}\right) - \exp\left(-\frac{t+T_d}{\tau}\right)\right] \tag{50}$$

The third integral is

$$\int_{t+\Delta t+T_d}^{t^{**}} a_3(t^*)\,dt^* = \bar{b} \times [a_c(t)](t^{**}-t-\Delta t-T_d) - \tau H_3 \times \left[\exp\left(-\frac{t^{**}}{\tau}\right) - \exp\left(-\frac{t+\Delta t+T_d}{\tau}\right)\right] \tag{51}$$

And so Eq. (48) becomes

$$\delta v(t^{**}) = H_4 + \bar{b} \times [a_c(t)] \times (t^{**}-t-\Delta t-T_d) - \tau H_3 \exp\left(-\frac{t^{**}}{\tau}\right) \tag{52}$$

where

$$H_4 = [a_c(t-\Delta t)]T_d + [a_c(t)]\Delta t + \tau \times \left[H_1 \exp\left(-\frac{t}{T}\right) + (H_2 - H_1)\exp\left(-\frac{t+T_d}{\tau}\right) + (H_3 - H_2)\exp\left(-\frac{t+\Delta t+T_d}{\tau}\right)\right] \tag{53}$$

Substituting Eqs. (38), (42), and (47) into Eq. (53) produces the simplification

$$H_4 = [a_c(t-\Delta t)](T_d+\tau) + [a_c(t)][\Delta t + (b-1)\tau] + \tau \times [a(t-\Delta t+T_d) - a_c(t-\Delta t)]\exp\left(\frac{T_d-\Delta t}{\tau}\right) \tag{54}$$

The generalized air-path axes position increment produced by divert action over the interval $(t, t+T)$ is, from Eq. (52),

$$\delta p(t+T) = \int_t^{t+T} \delta v(t^{**})\,dt^{**} = \{H_4 - \bar{b} \times [a_c(t)](t+\Delta t+T_d)\}T + \bar{b} \times [a_c(t)]\left[(t+T)^2 - t^2\right]/2 + \tau^2 H_3 \times \left[\exp\left(-\frac{t+T}{\tau}\right) - \exp\left(-\frac{t}{T}\right)\right] \tag{55}$$

If the desired value of $\delta p(t+T)$ is known, one may solve for $a_c(t)$. First, denote by $\varepsilon'(t_{f_B})$ the air-path axes steering correction needed to null the miss distance. Then, reassemble Eq. (55) by substitution of $\varepsilon'(t_{f_B})$ for $\delta p(t+T)$ and Eqs. (54), (47), (42), and (38):

$$\varepsilon'(t_{f_B}) = T[G_0(t) + G_1 a_c(t)] + \tfrac{1}{2}T^2\bar{b}a_c(t) + \tau^2[G_2(t,T) + G_3(t,T)a_c(t)] \tag{56}$$

where the prime in $\varepsilon'(t_{f_B})$ denotes air-path axes; $G_0(t)$, G_1, $G_2(t,T)$, and $G_3(t,T)$ are independent of $a_c(t)$ and are defined as

$$G_0(t) \equiv [a_c(t-\Delta t)](T_d+\tau) + \tau \times [a(t-\Delta t+T_d) - a_c(t-\Delta t)]\exp\left(\frac{T_d-\Delta t}{\tau}\right) \tag{57}$$

$$G_1 \equiv \Delta t + (b-1)\tau - \bar{b}\times(\Delta t + T_d) \tag{58}$$

$$G_2(t,T) \equiv \left\{[a_c(t-\Delta t)]\exp\left(\frac{t+T_d}{\tau}\right) + [a(t-\Delta t+T_d) - a_c(t-\Delta t)]\exp\left(\frac{t-\Delta t+T_d}{\tau}\right)\right\} \times \left[\exp\left(-\frac{t+T}{\tau}\right) - \exp\left(-\frac{t}{T}\right)\right] \tag{59}$$

$$G_3(t,T) \equiv \left[b\exp\left(\frac{t+\Delta t+T_d}{\tau}\right) - \exp\left(\frac{t+T_d}{\tau}\right)\right] \times \left[\exp\left(-\frac{t+T}{\tau}\right) - \exp\left(-\frac{t}{T}\right)\right] \tag{60}$$

Solving Eq. (56) for $a_c(t)$, one obtains

$$a_c(t) = \frac{\varepsilon'(t_{f_B}) - TG_0(t) - \tau^2 G_2(t,T)}{TG_1 + \tfrac{1}{2}T^2\bar{b} + \tau^2 G_3(t,T)} \tag{61}$$

where $a_c(t)$ and $\varepsilon'(t_{f_B})$ denote, in turn, the components of the acceleration command and predicted ballistic (zero-effort) miss distance projected along 1) the guided-vehicle drag axis, 2) sideforce axis, and 3) lift axis. The other terms in Eq. (61) incorporate the compensation required for dynamic inversion of the behavior of the reduced-order model of the guided-vehicle autopilot loop, given the engagement time to go T. The required guidance correction within the ECEF coordinate system is, from Eq. (36),

$$\underline{\varepsilon}'(t_{f_B}) = \underline{\Delta x}(t) + T\underline{\Delta \dot{x}}(t) + \tfrac{1}{2}T^2\underline{\ddot{x}}_{T_B}(t) - \tfrac{1}{2}T^2\underline{\ddot{x}}_{P_B}(t+T) + \underline{\delta x}_{T_B}(t+T) - \underline{\delta x}_{P_B}(t+T) \tag{62}$$

This correction is dependent upon the guided-vehicle accelerations along its air-path drag, sideforce, and lift axes, even though drag usually is not controllable independently.

We shall now examine further the last four terms in Eq. (62). For the target

$$\underline{\ddot{x}}_{T_B}(t) = \underline{F}_{0_T}(t) + \frac{q_T(t)S_T}{m_T}\underline{\underline{F}}_T(t)\begin{bmatrix} C_{D_T} \\ C_{N_{\alpha_T}}\alpha_T \sin(\sigma t+\Omega) \\ C_{N_{\alpha_T}}\alpha_T \cos(\sigma t+\Omega)\end{bmatrix} \tag{63}$$

For the guided vehicle, assuming constant axial force and zero lift and side forces over the interval $(t, t+T)$,

$$\underline{\dot{x}}_{P_B}(t) = \underline{F}_{0_P}(t) + \frac{q_P(t)S_P}{m_P(t)}\underline{\underline{F}}_P(t)\begin{bmatrix} C_A(t) \\ 0 \\ 0\end{bmatrix} \tag{64}$$

Changes in the axial force over $(t, t+T)$ and other high-order effects produce a nonzero $\underline{\delta x}_{T_B}(t+T)$. However, as $T \to 0$, the values of both of the differential ballistic acceleration correction terms over the path to go, $\underline{\delta x}_{T_B}(t+T)$ and $\underline{\delta x}_{P_B}(t+T)$, become negligible. For an end-game steering law employing feedback, i.e., a sequence of corrections, it is usually permissible to neglect these terms. (The results summarized in Sec. IV were obtained with these terms ignored.)

Thus,

$$\underline{\varepsilon}'(t_{f_B}) = \underline{\underline{F}}_P^{-1}\underline{\varepsilon}(t_{f_B}) \triangleq \underline{\underline{F}}_P^{-1}\left\{\underline{\Delta x}(t) + T\underline{\Delta \dot{x}}(t) + \tfrac{1}{2}T^2\left[\underline{F}_{0_T}(t) - \underline{F}_{0_P}(t)\right] + \tfrac{1}{2}T^2\frac{q_T(t)S_T}{m_T}\underline{\underline{F}}_T(t)\begin{bmatrix} C_{D_T} \\ C_{N_{\alpha_T}}\alpha_T\sin(\sigma t+\Omega) \\ C_{N_{\alpha_T}}\alpha_T\cos(\sigma t+\Omega)\end{bmatrix}\right\} - \tfrac{1}{2}T^2\frac{q_P(t)S_P}{m_P}\begin{bmatrix} C_A(t) \\ 0 \\ 0\end{bmatrix} \tag{65}$$

and therefore, expressing $a_c(t)$ in terms of its components along guided-vehicle drag, sideforce, and lift axes, respectively,

$$a_{D_c}(t) = K\times\left[f_{11_P}(t)\tilde{\varepsilon}_1(t_{f_B}) + f_{21_P}(t)\tilde{\varepsilon}_2(t_{f_B}) + f_{31_P}(t)\tilde{\varepsilon}_3(t_{f_B}) - TG_{0_D}(t) - \tau^2 G_{2_D}(t,T) - \tfrac{1}{2}T^2\frac{q_P(t)S_P C_A(t)}{m_P}\right] \tag{66}$$

$$a_{Y_c}(t) = K\times\left[f_{12_P}(t)\tilde{\varepsilon}_1(t_{f_B}) + f_{22_P}(t)\tilde{\varepsilon}_2(t_{f_B}) + f_{32_P}(t)\tilde{\varepsilon}_3(t_{f_B}) - TG_{0_Y}(t) - \tau^2 G_{2_Y}(t,T)\right] \tag{67}$$

$$a_{L_c}(t) = K\times\left[f_{13_P}(t)\tilde{\varepsilon}_1(t_{f_B}) + f_{23_P}(t)\tilde{\varepsilon}_2(t_{f_B}) + f_{33_P}(t)\tilde{\varepsilon}_3(t_{f_B}) - TG_{0_L}(t) - \tau^2 G_{2_L}(t,T)\right] \tag{68}$$

where

$$\tilde{\varepsilon}_i(t_{f_B}) = \Delta x_i(t) + T\Delta\dot{x}_i(t) + \tfrac{1}{2}T^2\left[F_{i_{0_T}}(t) - F_{i_{0_P}}(t)\right] + \tfrac{1}{2}T^2\frac{q_T(t)S_T}{m_T}\left\{f_{i1_T}(t)C_{D_T} + f_{i2_T}(t)\left[C_{N_{\alpha_T}}\alpha_T\sin(\sigma t+\Omega)\right] + f_{i3_T}(t)[C_{N_{\alpha_T}}\alpha_T\cos(\sigma t+\Omega)]\right\} \tag{69}$$

and the gain K is defined as

$$K = 1/\left[TG_1 + \tfrac{1}{2}T^2\bar{b} + \tau^2 G_3(t,T)\right] \tag{70}$$

Note that $\tilde{\varepsilon}_i(t_{f_B})$ excludes the effect of the $C_A(t)$ term, which (for small α and β) influences $a_{D_c}(t)$ only.

Eqs. (66–68) are roughly analogous in function to Eqs. (13) and (26) of Sec. I. As before, an estimate of T is needed. If $a_{D_c}(t)$ is zero, the steering command is perpendicular to the instantaneous velocity vector $\underline{V}_P(t)$ and therefore satisfies Eq. (14), whence Eq. (24) is again the solution for T. However, there usually is no physical mechanism for independent realization of $a_{D_c}(t)$. Moreover, because of induced drag, acceleration of the guided vehicle along its drag axis has a power-law dependence on $a_{Y_P}(t)$ and $a_{L_P}(t)$, as shown in Appendix B. Should the estimate of T be modified to account for nonzero $a_{D_P}(t)$?

The calculated $a_{Y_c}(t)$ and $a_{L_c}(t)$, Eqs. (67 and 68), imply a resultant velocity divert angle $\eta(t)$. If one uses formulation A, the approximate error in $\eta(t)$ that results from an error ε_T in estimating T is

$$\varepsilon_\eta \doteq \frac{\varepsilon_T\left[a_{Y_c}^2(t) + a_{L_c}^2(t)\right]^{\frac{1}{2}}}{V_P(t)}$$

But the contribution of $a_{D_P}(t)$ to ε_T is approximately

$$\varepsilon_T \doteq \frac{\|\underline{\Delta x}(t)\|}{V_P(t) + Ta_{D_P}(t)} - \frac{\|\underline{\Delta x}(t)\|}{V_P(t)} = -\frac{T^2 a_{D_P}(t)}{V_P(t)}$$

and therefore

$$\varepsilon_\eta \doteq -\frac{T^2 a_{D_P}(t)}{V_P^2(t)}\left[a_{Y_c}^2(t) + a_{L_c}^2(t)\right]^{\frac{1}{2}}$$

The miss distance produced by a single steering correction (not feedback law) for which the estimate of T neglects the effect of $a_{D_P}(t)$ is thus approximately

$$\delta(t, T) \doteq \varepsilon_\eta T V_P(t) \doteq -\frac{T^3 a_{D_P}(t)\left[a_{Y_c}^2(t) + a_{L_c}^2(t)\right]^{\frac{1}{2}}}{V_P(t)} \tag{71}$$

where

$$a_{D_P}(t) = f_{11_P}(t)F_{1_{0_P}}(t) + f_{21_P}(t)F_{2_{0_P}}(t) + f_{31_P}(t)F_{3_{0_P}}(t) + \frac{q_P(t)S_P C_A(t)}{m_P} + \frac{K_N(t)m_P\left[a_{Y_c}^2(t) + a_{L_c}^2(t)\right]}{q_P(t)S_P[K_N(t) - C_A(t)]} \tag{72}$$

These equations can help one determine if the value of T estimated via Eq. (24) will be sufficiently accurate. Note that with Eq. (24) the estimated T is usually slightly greater than the actual T, producing a small tendency for the RCEG steering commands to be weaker than their ideal values. With a feedback form of guidance law this should not be a serious problem.

However, to consider more precisely the effect of $a_{D_P}(t)$ on T, one may derive the second integral of the component of guided-vehicle acceleration response acting along its drag axis subsequent to a divert command issued at t:

$$\delta_D(t, T) = E_P(t)\Big\{T\Big[J_{1a_Y} + J_{1a_L} + J_{1b_Y}\cdot a_{Y_c}(t) + J_{1b_L}\cdot a_{L_c}(t) + J_{1c_Y}\cdot a_{Y_c}^2(t) + J_{1c_L}\cdot a_{L_c}^2(t)\Big] + \tfrac{1}{2}T^2\Big[J_{2a_Y} + J_{2a_L} + J_{2b_Y}\cdot a_{Y_c}(t) + J_{2b_L}\cdot a_{L_c}(t) + J_{2c_Y}\cdot a_{Y_c}^2(t) + J_{2c_L}\cdot a_{L_c}^2(t)\Big]\Big\} \tag{73}$$

for which the parameter groups are defined in Appendix B. To a first approximation

$$\varepsilon_T \doteq \delta_D(t, T)/V_P(t) \tag{74}$$

and thus one may use as a more accurate estimate of the time to go

$$T = [T\text{from Eq. (24)}] - [\varepsilon_T\text{from Eq. (74) using } T \text{ from Eq. (24)}] \tag{75}$$

IV. Simulation Results

The RCEG steering laws of Secs. II and III have been evaluated in closed-loop simulations involving ballistic, coning ballistic, and boosted targets. It has been found that versions of the simple case treated in Sec. II are appropriate for exo-atmospheric engagements in which the guided vehicle employs on-off reaction motors for its divert maneuvers.

The general case treated in Sec. III is appropriate for endo-atmospheric intercepts. Use of formulation B from Sec. III, with time to go computed from Eq. (24), has been evaluated for a notional hypervelocity endo-atmospheric projectile of a type suitable for defense against strategic and theater missile threats. The results of this evaluation are summarized next. The simulated endo-atmospheric projectile is a command-guided kinetic kill vehicle that would be gun or rocket launched to an initial speed of 2–4 km/s. It would be unpropelled during its guidance maneuvers and would employ aerodynamic maneuvering. Classical guidance laws, such as pure proportional navigation, were simulated but did not meet the terminal accuracy requirement in this application.

The RCEG steering law was installed in a detailed six-degree-of-freedom simulation, ENDOSIM,[10] used for the Strategic Defense Initiative (SDI) and other interceptor guidance-law evaluations, and an independent test of the RCEG law was performed using the preceding projectile characteristics and hypothetical parameters for a pure-ballistic re-entry target. Fifty Monte Carlo simulation runs were computed for each of three nominal intercept conditions. These runs had different timing errors associated with turn on and turn off of the autopilot reaction control thrusters in the guided vehicle. The timing errors had a standard deviation of 0.3 ms. The nominal intercept conditions are given in Table 1.

Table 1 Nominal intercept conditions

Scenario	Downrange, km	Crossrange, km	Altitude, km	Crossing angle at intercept, deg
1	10	0	8	Nil
2	9	15	8	30
3	18	0	18	Nil

Table 2 Miss-distance statistics for RCEG law and a simplified IPG guidance law

	Mean distance		Standard deviation of distance	
Scenario	RCEG	IPG	RCEG	IPG
1	3.08	3.26	2.12	2.15
2	4.96	4.75	2.74	2.72
3	9.23	9.51	8.18	8.81

The miss-distance statistics for the RCEG law and a simplified IPG guidance law for the same Monte Carlo tests are given in arbitrary units in Table 2. It is believed that neglected error sources do not affect these comparative results.

All of the simulation runs used a high-order, nonlinear simulation of the projectile and its actuation subsystem. The parameter values in the RCEG law were an assumed transport delay T_d of 0.010 s and an assumed autopilot-loop time constant τ of 0.065 s. Both end-game steering laws were invoked for the final 1.0 s of each intercept and used a command update interval Δt of 0.010 s. The predictive guidance law (simplified IPG) used in this comparison did not employ iteration at the time of decision but over successive decisions. It made a translational three-degree-of-freedom predicted-miss calculation via numerical integration at each guidance update, assuming continuation of the acceleration command calculated from the immediate prior time of update. (For the first guidance interval, the prior command was taken as zero.)

The RCEG steering law required a computational throughput approximately 36 times less than that of the simplified IPG law.

Separate tests of the robustness of the RCEG law were made by the author and a colleague using the lumped-parameter model of the autopilot loop in a three-degree-of-freedom point-mass simulation of the hypothetical projectile. With the aforementioned parameter settings in the RCEG law, its accuracy was largely insensitive to off-nominal values of the projectile autopilot parameters as long as those parameters were confined to the following simultaneous (random three-parameter variations) ranges of variation: 0.005 s $\leq T_d \leq$ 0.020 s, 0.040 s $\leq \tau \leq$ 0.100 s, and $\Delta t \leq$ 0.024 s. The simplified IPG accuracy deteriorated for $\Delta t >$ 0.010 s, and the RCEG law accuracy deteriorated for $\Delta t >$ 0.024 s. Thus, the RCEG law allows use of a larger update interval.

The heavy computational load associated with IPG laws adds to the guidance loop delay T_d, and this in turn would degrade performance using IPG. On the other hand, the reduced computation requirement of the RCEG law allows it to operate with a minimum T_d (reviewer).

The sensitivity of RCEG law miss distance to initial heading error, crossing angle, maneuver g limit of the guided vehicle, and end-game time have not been investigated. It is believed that these are comparable to the IPG law sensitivities for small end-game time (1.0 s or less in the present example).

V. Conclusions

RCEG exo-atmospheric and endo-atmospheric steering laws have been derived analytically in closed form to reduce the computational burden for accurate predictive guidance of high-performance weapon systems. The RCEG formulation provided a throughput

reduction of approximately 36:1 relative to a simplified form of IPG. Monte Carlo and other simulation tests have verified that the RCEG steering laws are competitive in miss distance with an iterative predictive guidance (IPG) algorithm requiring substantially more computation and are robust in the presence of off-nominal characteristics of the guided vehicle. State estimation errors have not been considered. The derivation of the endo-atmospheric RCEG laws also incorporates a provision for efficiently coping with target trajectory oscillations of the type produced by "coning" rotational motion of the target vehicle.

Appendix A: Elaboration on Endo-Atmospheric Equations of Motion

The vector $\underline{F}_0$ appearing in Eq. (29) has the components

$$F_{0_1} = 2\omega_E \dot{x}_2 + \omega_E^2 x_1 - k_{111} g \tag{A1}$$

$$F_{0_2} = -2\omega_E \dot{x}_1 + \omega_E^2 x_2 - k_{211} g \tag{A2}$$

$$F_{0_3} = -k_{311} g \tag{A3}$$

The matrix $\underline{\underline{F}}$ in Eq. (29) is

$$\underline{\underline{F}} = \begin{bmatrix} f_{11} & f_{12} & f_{13} \\ f_{21} & f_{22} & f_{23} \\ f_{31} & f_{32} & f_{33} \end{bmatrix} \tag{A4}$$

in which

$$f_{11} = -k_{111} \sin\gamma - k_{112} \cos\gamma \tag{A5}$$

$$f_{12} = k_{110} \tag{A6}$$

$$f_{13} = -k_{112} \sin\gamma + k_{111} \cos\gamma \tag{A7}$$

$$f_{21} = -k_{211} \sin\gamma - k_{212} \cos\gamma \tag{A8}$$

$$f_{22} = k_{220} \tag{A9}$$

$$f_{23} = -k_{212} \sin\gamma + k_{211} \cos\gamma \tag{A10}$$

$$f_{31} = -k_{311} \sin\gamma - k_{312} \cos\gamma \tag{A11}$$

$$f_{32} = k_{330} \tag{A12}$$

$$f_{33} = -k_{312} \sin\gamma + k_{311} \cos\gamma \tag{A13}$$

where γ is measured positive upwards.

The k_{ijk} parameter groups are

$$k_{111} = \cos\Lambda \cos\lambda \tag{A14}$$

$$k_{112} = -\cos\Lambda \sin\lambda \cos\chi - \sin\Lambda \sin\chi \tag{A15}$$

$$k_{110} = \cos\Lambda \sin\lambda \sin\chi - \sin\Lambda \cos\chi \tag{A16}$$

$$k_{211} = \sin\Lambda \cos\lambda \tag{A17}$$

$$k_{212} = -\sin\Lambda \sin\lambda \cos\chi + \cos\Lambda \sin\chi \tag{A18}$$

$$k_{220} = \sin\Lambda \sin\lambda \sin\chi + \cos\Lambda \cos\chi \tag{A19}$$

$$k_{311} = \sin\lambda \tag{A20}$$

$$k_{312} = \cos\lambda \cos\chi \tag{A21}$$

$$k_{330} = -\cos\lambda \sin\chi \tag{A22}$$

where $\Lambda = \tan^{-1}(x_2/x_1)$, $\lambda = \tan^{-1}[x_3/(x_1^2 + x_2^2)^{\frac{1}{2}}]$, and χ is measured positive to the East of North.

Appendix B: Procedure for Treating Effects of Axial Acceleration Changes over the T Interval

Steering maneuvers produce induced forces along the guided-vehicle drag axis, and these forces can influence the time to go T. Assuming that q_P, m_P, C_A, K_N, and $\underline{\underline{F}}_P$ are constant during the end-game time to go, one may model the induced drag approximately via the squares of a_Y and a_L, thus obtaining Eq. (73), in which

$$J_{1a} = H_{5a} - \frac{\tau}{2} H_{3a}^2 \exp\left(-\frac{2t}{\tau}\right) \tag{B1}$$

$$J_{1b} = H_{5b} - 2\tau \bar{b} H_{3a} \exp\left(-\frac{t}{T}\right) - \tau H_{3a} H_{3b} \exp\left(-\frac{2t}{\tau}\right) \tag{B2}$$

$$J_{1c} = H_{5c} + \bar{b}t - 2\tau \bar{b} H_{3b} \exp\left(-\frac{t}{T}\right) - \frac{\tau}{2} H_{3b}^2 \exp\left(-\frac{2t}{\tau}\right) \tag{B3}$$

$$J_{2a} = H_{3a}^2 \exp\left(-\frac{2t}{\tau}\right) \tag{B4}$$

$$J_{2b} = 2\bar{b} H_{3a} \exp\left(-\frac{t}{T}\right) + 2H_{3a} H_{3b} \exp\left(-\frac{2t}{\tau}\right) \tag{B5}$$

$$J_{2c} = \bar{b} \times \left[1 + 2H_{3b} \exp\left(-\frac{t}{T}\right)\right] + H_{3b}^2 \exp\left(-\frac{2t}{\tau}\right) \tag{B6}$$

wherein

$$H_{3a} = H_1 + a_c(t - \Delta t) \times \exp\left(\tfrac{t+T_d}{\tau}\right) \tag{B7}$$

$$H_{3b} = \exp\left(\tfrac{t+T_d}{\tau}\right)\left[b \times \exp\left(\tfrac{\Delta t}{\tau}\right) - 1\right] \tag{B8}$$

$$\begin{aligned} H_{5a} = {} & a_c^2(t - \Delta t) \times T_d \\ & - \tau \times \left\{ 2a_c(t - \Delta t) \times H_1 \exp\left(-\frac{t}{T}\right)\left[\exp\left(-\frac{T_d}{\tau}\right) - 1\right] \right. \\ & + \tfrac{1}{2} H_1^2 \exp\left(-\frac{2t}{\tau}\right)\left[\exp\left(-\frac{2T_d}{\tau}\right) - 1\right] \\ & + \tfrac{1}{2}\left[H_1 + a_c(t - \Delta t) \times \exp\left(\frac{t + T_d}{\tau}\right)\right]^2 \\ & \times \exp\left(-\frac{2t + 2T_d}{\tau}\right)\left[\exp\left(-\frac{2\Delta t}{\tau}\right) - 1\right] \\ & \left. - \tfrac{1}{2} H_{3a}^2 \exp\left(-\frac{2t + 2\Delta t + 2T_d}{\tau}\right)\right\} \end{aligned} \tag{B9}$$

$$\begin{aligned} H_{5b} = {} & -\tau \times \left\{ 2\left[H_1 + a_c(t - \Delta t) \times \exp\left(\frac{t + T_d}{\tau}\right)\right] \right. \\ & \times \exp\left(-\frac{t + T_d}{\tau}\right)\left[\exp\left(-\frac{\Delta t}{\tau}\right) - 1\right] \\ & - \left[H_1 + a_c(t - \Delta t) \times \exp\left(\frac{t + T_d}{\tau}\right)\right] \\ & \times \exp\left(-\frac{t + T_d}{\tau}\right)\left[\exp\left(-\frac{2\Delta t}{\tau}\right) - 1\right] \\ & - 2\bar{b} H_{3a} \exp\left(-\frac{t + \Delta t + T_d}{\tau}\right) \\ & \left. - H_{3a} H_{3b} \exp\left(-\frac{2t + 2\Delta t + 2T_d}{\tau}\right)\right\} \end{aligned} \tag{B10}$$

$$H_{5c} = \Delta t - \bar{b}\,(t + \Delta t + T_d)$$
$$+ \tau \times \left\{ 2\left[\exp\left(-\frac{\Delta t}{\tau}\right) - 1\right] - \tfrac{1}{2}\left[\exp\left(-\frac{2\Delta t}{\tau}\right) - 1\right] \right.$$
$$+ 2\bar{b}H_{3b}\exp\left(-\frac{t + \Delta t + T_d}{\tau}\right)$$
$$\left. + \tfrac{1}{2}H_{3b}^2\exp\left(-\frac{2t + 2\Delta t + 2T_d}{\tau}\right)\right\} \tag{B11}$$

Accordingly, the second integral of the acceleration response of the guided vehicle to a steering command at t is

$$\underline{\delta x}_P(t+T) \doteq \underline{\underline{F}}_P(t) \begin{Bmatrix} E_P(t)\{\bullet\} \\ T\left[G_{0_Y} + G_1 a_{Y_c}(t)\right] + \tfrac{1}{2}T^2\bar{b}a_{Y_c}(t) \\ T\left[G_{0_L} + G_1 a_{L_c}(t)\right] + \tfrac{1}{2}T^2\bar{b}a_{L_c}(t) \end{Bmatrix} \tag{B12}$$

where $\{\bullet\}$ is the bracketted expression in Eq. (73)

Acknowledgments

The work on which this paper is based was supported by Technovative Applications (Brea, California) under its Contract DASG60-91-C-0105 (Phase II) with the United States Army Strategic Defense Command. The author gratefully acknowledges the contributions of James K. Williams, program manager for Technovative Applications; C. Thomas Alexander of Amtec Corporation (Huntsville, Alabama), who checked the derivation, programmed and performed the Monte Carlo simulation studies of RCEG and simplified IPG steering law accuracies, and calculated the throughput comparisons; Natalie A. Nigro of Barron Associates, who performed the simulation study of robustness; and David G. Ward of Barron Associates, who discussed ideas with the author. The author also acknowledges the many helpful suggestions by the reviewers and editor of this paper.

References

[1]Zarchan, P., *Tactical and Strategic Missile Guidance*, Vol. 124, Progress in Astronautics and Aeronautics, AIAA, Washington, DC, 1990, pp. 308–317.

[2]Kim, Y. S., Cho, H. S., and Bien, Z., "A New Guidance Law for Homing Missiles," *Journal of Guidance, Control, and Dynamics*, Vol. 8, No. 3, 1985, pp. 402–404.

[3]Looze, D. P., Hsu, J. Y., and Grunberg, D., "Investigation of the Use of Acceleration Estimates by Endgame Guidance Laws," *Journal of Guidance, Control, and Dynamics*, Vol. 13, No. 2, 1990, pp. 198–206.

[4]Cochran, J. E., Jr., No, T. S., and Thaxton, D. G., "Analytical Solutions to a Guidance Problem," *Journal of Guidance, Control, and Dynamics*, Vol. 14, No. 1, 1991, pp. 117–122.

[5]Baba, Y., Yamaguchi, M., and Howe, R. M., "Generalized Guidance Law for Collision Courses," *Journal of Guidance, Control, and Dynamics*, Vol. 16, No. 3, 1993, pp. 511–516.

[6]Lee, G. K. F., "Estimation of the Time-to-Go Parameter for Air-to-Air Missiles," *Journal of Guidance, Control, and Dynamics*, Vol. 8, No. 2, 1985, pp. 262–266.

[7]Hull, D. G., Radke, J. J., and Mack, R. E., "Time-to-Go Prediction for Homing Missiles Based on Minimum-Time Intercepts," *Journal of Guidance, Control, and Dynamics*, Vol. 14, No. 2, 1991, pp. 865–871.

[8]Barron, A. R., and Barron, R. L., "Statistical Learning Networks: A Unifying View," *Computing Science and Statistics: Proceedings of the 20th Symposium on the Interface*, edited by E. Wegman, American Statistical Association, Alexandria, VA, 1988, pp. 192–203.

[9]Poggio, T., and Girosi, F., "Networks for Approximation and Learning," *Proceedings of the IEEE*, Vol. 78, No. 9, 1990, pp. 1481–1497.

[10]Anon., "Comprehensive Example Report, ENDOSIM Version 2.1," Amtec Corp., U.S. Army Contract DASG60-84-C-097, Huntsville, AL, Aug. 1989.